P-P and As-As isovalent impurity pairs in GaN: Interaction of deep t_2 levels

T. Mattila* and Alex Zunger†
National Renewable Energy Laboratory, Golden, Colorado 80401
(Received 9 April 1998)

The electronic and atomic structure of substitutional nth neighbor ($1 \leqslant n \leqslant 6$) P-P and As-As impurity pairs in zinc blende GaN is investigated using self-consistent plane-wave pseudopotential and empirical pseudopotential methods. A single impurity introduces a deep t_2 gap level; we show that the interaction between the t_2 defect orbitals of the impurity pairs leads to an interesting pattern of single-particle level splitting, being largest for the first ($n=1$) and fourth ($n=4$) neighbor pairs, both exhibiting a C_{2v} symmetry. The total energy of the nth order pair $\Delta E^{(n)}$ relative to isolated ($n \to \infty$) impurities indicates pairing tendency for $n=1$ and $n=2$ ($\Delta E^{(1,2)}<0$) while $n=4$ pairs are unstable ($\Delta E^{(4)}>0$). We explain this behavior of $\Delta E^{(n)}$ vs n as a consequence of the interplay between two effects: an ''elastic contribution'' representing the interaction between the elastic strain fields of the two impurities and an ''electronic contribution'' describing the interaction of the defect orbitals of the two impurity atoms. The binding energies of the impurity-pair bound excitons are calculated for the $n=1$ As-As and P-P pairs and are found to be significantly larger than for the corresponding isolated impurities. The probabilities for electronic transitions between the defect levels and conduction band are calculated. The results predict existence of a rich series of spectroscopic features distinct from single impurities. [S0163-1829(99)14415-1]

I. INTRODUCTION

There exists significant interest[1–6] in the mixed *anion* nitride alloys $GaAs_xN_{1-x}$ and GaP_xN_{1-x}. It has been shown experimentally that incorporation of As in GaN is possible in the concentration range 10^{17}–10^{18} 1/cm.[1,2]. The dilute limit at the N-rich end of these alloys corresponds to P or As impurities in GaN (denoted GaN:P and GaN:As). These isovalent impurities are of great experimental interest as they decide the optical properties of the alloy. The early work performed by Pankove and Hutchby,[7] Metcalfe *et al.*,[8] and Ogino and Aoki[9] identified luminescence peaks well below the band gap in GaN samples containing P or As. Recent spectroscopic studies have indeed confirmed that P and As induce deep states in the GaN band gap: Li *et al.*[1] have used cathodolumiscence measurements to characterize the deep As-related emission, Guido *et al.*[2] have indicated significant enhancement in electron mobility and integrated photoluminescence due to As doping of GaN, and Jadwisienczak and Lozykowski[3] have determined the detailed photoluminescence characteristics (e.g., the exciton binding energies) of P and As deep centers. In agreement with these experimental studies, recent theoretical calculations[4–6] have shown that *isolated* GaN:P (GaN:As) induce a deep, threefold degenerate *p*-like (t_2) defect level $\sim$0.6 eV ($\sim$0.75 eV) above the valence band maximum, which acts as the origin of the observed luminescence transitions.

In a dilute alloy, the limited solubility leads to clustering of solute atoms, the simplest form being *impurity pairing*. The spectroscopic consequences of pairing have been studied in detail for systems where at the *isolated* impurity limit one has an *s*-like (a_1) gap level; an example is the isovalent nitrogen impurity in GaP (denoted GaP:N).[10,11] Indeed, such a_1-a_1 pairing leads to a very rich series of spectroscopic lines whose position is determined by the intrapair atomic distance.[10,11] As the isolated P and As impurities in GaN induce a *p*-like (t_2) deep level,[4–6] the purpose of this paper is to study the consequences of the t_2-t_2 interaction of the P-P and As-As impurity pairs. We consider nth P-P and As-As neighbor pairs in zinc blende GaN in the nitrogen fcc sublattice with $n=1,2,3,4,5,6$, illustrated in Fig. 1. We have chosen the zinc blende structure (instead of wurtzite) to allow an easier comparison with the known case of nitrogen impurities in zinc blende GaP.[10,11] Specifically we list the following.

(i) We calculate the relaxed equilibrium atomic geometries and analyze the resulting atomic symmetries of the impurity pairs. We find the point symmetry groups C_{2v}, D_{2d}, C_s, C_{2v}, C_2, and C_{3v} for $n=1,2,3,4,5,6$, respectively.

(ii) We study the interaction between the t_2 deep levels in these reduced symmetry atomic geometries. We show that

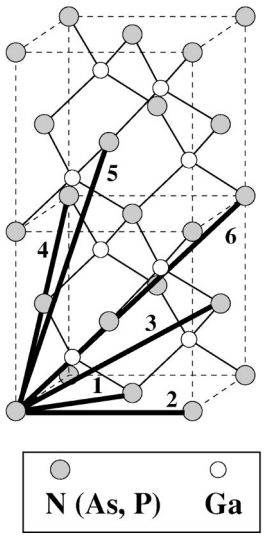

FIG. 1. The six first ($n=1,2,\ldots,6$) neighbor pair configurations in the nitrogen fcc sublattice of zinc blende GaN.

TABLE I. Atomic position of the first to sixth neighbor impurity atom ($n=1,2,3,4,5,6$) relative to an impurity atom located at the origin. In each case we give an example of the Cartesian coordinates (x_n, y_n, z_n) of the other constituent of the pair. The distance between the two impurities in each pair is given by $d_n = \sqrt{2n}/2\ a_0$. All values are given in units of the lattice constant a_0. The point group symmetries for the pairs (Ref. 11) are listed in the last column.

n	Position $(x_n, y_n, z_n)/a_0$	Distance d_n/a_0	Point group symmetry
1	(1/2,1/2,0)	$1/\sqrt{2}$	C_{2v}
2	(1,0,0)	1	D_{2d}
3	(1,1/2,1/2)	$\sqrt{6}/2$	C_s
4	(1,1,0)	$\sqrt{2}$	C_{2v}
5	(3/2,1/2,0)	$\sqrt{10}/2$	C_2
6	(1,1,1)	$\sqrt{3}$	C_{3v}

t_2-t_2 interaction leads to interesting defect level splitting which depends strongly on the pair symmetry and atomic separation. The largest splitting and complete removal of the orbital degeneracy is predicted for $n=1$ and $n=4$ pairs, both exhibiting C_{2v} symmetry, while for $n=2$ with D_{2d} symmetry we find only a partial removal of the degeneracy, and a small splitting.

(iii) The transition probabilities for electronic excitations between the impurity-pair-induced defect levels and the lowest conduction band are found to be large. Since the transitions are energetically well separated from the transitions related to the isolated impurities, the presence of As-As and P-P impurity pairs in GaN should manifest itself via spectroscopic features that are distinct from those of the isolated impurities.

(iv) We calculate the exciton binding energies for nearest neighbor ($n=1$) As-As (P-P) pairs at $E_b=1.27\,(0.85)$ eV. These values are considerably larger than those calculated for isolated impurities [$E_b=0.41\,(0.22)$ eV for As (P)].[6]

(v) Having established the electronic and atomic structure of the impurity pairs we investigate their formation energy $\Delta E^{(n)}$, i.e., the energy of an nth neighbor impurity pair relative to the energy of two isolated impurities ($n\to\infty$). We decompose $\Delta E^{(n)}$ into two contributions: an elastic part resulting from the long-ranged interaction of the strain fields induced by the two impurities, and a chemical part representing the electronic interactions (in particular, the interaction induced by the deep t_2 defect orbitals). We show that both contributions depend strongly on the orientation of the impurity atoms relative to the lattice. We predict P-P and As-As *clustering* at nearest and next-nearest sublattice sites ($\Delta E^{(n)}<0$, for $n=1,2$), whereas the fourth neighbor configuration is unstable ($\Delta E^{(4)}>0$). For $n>4$ we find that $\Delta E^{(n)}$ is approaching zero, i.e., weak inter-impurity interaction.

II. METHODS

A. *Ab initio* and empirical pseudopotentials

In this study we will use two approaches, (i) the *ab initio* and (ii) the empirical pseudopotential methods, to investigate the atomic and electronic properties of the impurity pairs. With both methods we use supercells to simulate the defect pair placed in an infinite lattice. While an isolated point defect can be reliably studied with moderate size supercells (typically 64 atoms in the zinc blende structure), the study of impurity pairs requires the use of larger cells. This can be seen by considering the relative geometries for impurity pairs, representing the nth fcc neighbor ($n=1,2,3,4,5,6$) to each other in the zinc blende structure, described in Fig. 1 and Table I. It is evident that a 64 atom supercell ($2\times2\times2$ eight atom unit cells) becomes inadequate when $n>1$. This is due to the periodic boundary conditions which cause the distances between the actual impurity atoms (d_i in Table I) and their periodic images to become equal and thus impose artificial symmetry constraints. Furthermore, we will show below (Sec. III E) that the strain-mediated impurity-impurity interaction can be long ranged, and can thus require the use of large cells.

As a primary approach in this study we use the self-consistent plane-wave pseudopotential calculations,[12] based on density-functional theory within the local density approximation (LDA). The exchange-correlation term is parametrized as by Perdew and Zunger.[13] For nitrogen we use ultrasoft pseudopotential,[14] while for Ga, As, and P we use norm-conserving pseudopotentials[15] with the nonlinear core-valence exchange-correlation scheme[16] and s component as the local one. The Ga $3d$ orbitals are treated as part of the core.[17–19] A 25 Ry kinetic-energy cutoff is applied for the plane-wave basis, showing excellent convergence of the results with respect to the basis size. In the LDA calculations we use two system sizes: 64 and 216 atom supercells. The use of a 216 atom supercell is enabled by using a highly efficient parallel implementation of the method on the Cray T3E. The Brillouin zone sampling with the 64 atom cell size is done using a $2\times2\times2$ Monkhorst-Pack special k-point grid.[20] For the larger 216 atom cell only the Γ point is used. However, this sampling is accurate with such a large supercell as shown, e.g., in Ref. 21. The alignment of the screened local potential needed to determine the valence band maximum in the LDA defect calculations is done as in Ref. 6. However, when two impurities are present in the 64 atom supercell, the selection of a region inside the supercell where the potential is bulklike becomes difficult due to the influence of the nearby impurities. Therefore, we have approximated the magnitude of the effective potential alignment based on the results for isolated impurities. For the neutral impurity pair we use twice the value found for the corresponding neutral impurity. In the singly positive charge state of the impurity pair (used for estimation of the exciton bind-

TABLE II. The orbital energies (eV) of the deep impurity level and the relaxed bond length for *isolated* P and As impurities in GaN as calculated by LDA (64 atom cell) and EPM-VFF (512 atom cell) methods in Ref. 6. $R_{\text{Ga-}X}$ denotes the distance between the impurity and nearest-neighbor Ga atoms in units of the theoretical (Ref. 30) bond length ($R^0_{\text{Ga-N}}$) in bulk GaN.

X	Orbital energy (LDA)	Orbital energy (EPM)	$R_{\text{Ga-}X}/R^0_{\text{Ga-N}}$ (LDA)	$R_{\text{Ga-}X}/R^0_{\text{Ga-N}}$ (VFF)
As	$\epsilon_v+0.60$	$\epsilon_v+0.75$	1.155	1.151
P	$\epsilon_v+0.40$	$\epsilon_v+0.61$	1.132	1.131

ing energy) we use the isolated values for neutral and singly positive charge states added together. In the LDA calculations performed with 216 atom supercell (or empirical pseudopotential calculations with the 512 atom supercell described below) the alignment correction becomes negligible due to the large cell size. Further details of the LDA computational method can be found in Ref. 6.

Due to the band gap underestimation in LDA calculations,[22] optically more reliable single-particle levels can be obtained via empirical pseudopotential method (EPM).[4,5] The EPM employed in this study is identical with the one applied in Refs. 4 and 5. To briefly summarize, we first use the valence force field (VFF) method[23,24] to find the relaxed atomic positions. The electronic single-particle levels associated with these atomic structures are then calculated using specially fitted local pseudopotentials,[4] within a plane-wave basis. The Hamiltonian matrix is diagonalized via the folded spectrum method.[25] The advantage of this EPM based approach is that it predicts realistic band gaps and single-particle spectrum. This approach has been used[4,5,26] to obtain GaN-GaAs and GaN-GaP alloy structural parameters and optical properties, in agreement with experiment. Also, its computational effort scales linearly as a function of the system size. This allows us to easily study 512–1000 atom systems not accessible in LDA calculations. We next examine the consistency of the results between the LDA and EPM approaches.

B. Comparison of LDA and EPM results

Table II compares orbital energies of the gap levels obtained by the LDA and EPM for *isolated* P and As impurities in GaN.[6] Also, the relaxed atomic positions, calculated by the LDA and VFF methods, respectively, are given. We see a reasonable consistency between the results given by the two methods: The relaxed atomic geometries are within 0.3%. Both methods predict deep, threefold degenerate (t_2) deep defect levels in the band gap. The EPM-derived energy levels are slightly higher in energy with respect to the valence band maximum.

Figure 2(a) shows schematically the relaxed atomic geometry for the $n=1$ As-As *pair* in GaN. The relative bond lengths can be grouped into three distinct values denoted by *a*, *b*, and *c* [Fig. 2 (a)]. The comparison of these equilibrium anion-cation bond lengths (normalized to the Ga-N value in defect-free GaN) found in VFF and in LDA calculations is given in Table III. The values reveal again excellent agreement between VFF and LDA, and show outward relaxation

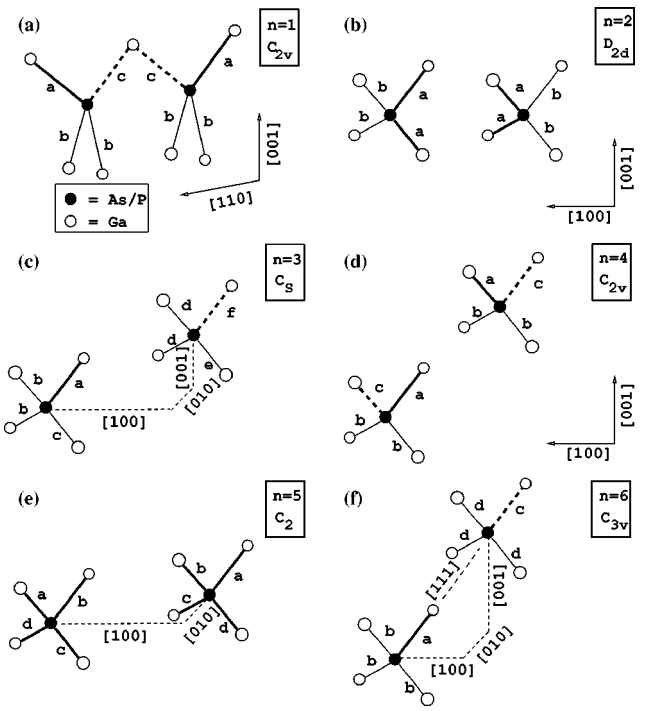

FIG. 2. Schematic presentation of the symmetry-inequivalent relaxed atomic geometries for the six As-As and P-P impurity pairs in GaN (Table I). The letters *a*, *b*, *c*, *d*, *e*, and *f* denote symmetry distinct bonds.

of the nearest neighbor Ga atoms surrounding the impurity, consistent with the results for isolated impurities.[6]

Figure 3 illustrates the single-particle levels found in the EPM and LDA calculations for the relaxed $n=1$ As-As pair. We see that the EPM and LDA methods produce nearly identical splitting of the degenerate levels associated with isolated impurities. However, as the band gap is underestimated in LDA calculations, the single-particle spectrum with respect to conduction band is much better reproduced by the EPM. We conclude that the EPM used here and the LDA method produce consistent results.

C. Choice of computational methods

Given (a) the similarity in the relaxed atomic configurations obtained by VFF and LDA, (b) the superiority of LDA in obtaining total energies (elastic + chemical contributions), and (c) the superiority of EPM in obtaining spectroscopically realistic level structure, the strategy we choose is

TABLE III. The relaxed relative anion-cation bond lengths $R^{\alpha}_{\text{Ga-As}}/R^0_{\text{Ga-N}}$ describing the atomic configuration of GaN crystal with the nearest-neighbor ($n=1$) As-As pair. Values obtained from LDA calculations with 64 atom supercell and VFF calculations with 512 atom supercells are given. The bond lengths are classified into three types $\alpha=a,b,c$ [see Fig. 2(a)]. The values are given relative to the theoretical Ga-N bond lengths in bulk GaN (Ref. 30).

Method and cell size	Relative bond length		
	Bond *a*	Bond *b*	Bond *c*
LDA (64)	1.147	1.157	1.158
VFF (512)	1.146	1.154	1.141

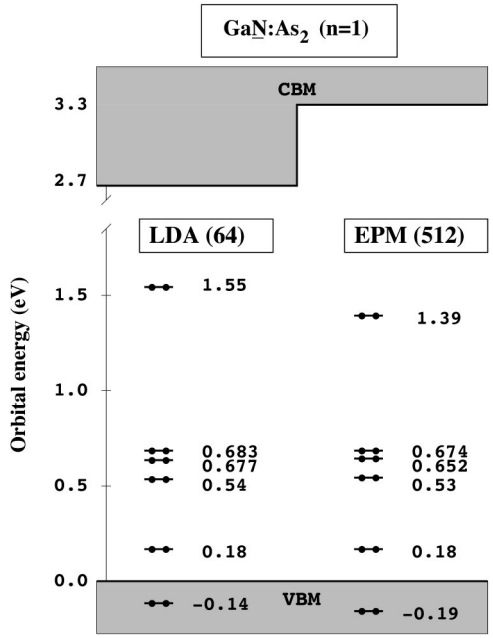

FIG. 3. The single-particle energy levels found in the EPM and LDA calculations for the relaxed first neighbor ($n=1$) As-As-impurity pair in GaN.

as follows (i) obtain the relaxed atomic geometries for the $n=1,2,3,4,5,6$ impurity pairs using either VFF or LDA methods, (ii) obtain the single-particle level splitting for the deep t_2 orbitals and the transition probabilities into the induced levels using large supercells and EPM, (iii) determine the impurity-pair bound exciton binding energies using LDA total energies obtainable for neutral and positive charge states, (iv) obtain the formation energies $\Delta E^{(n)}$ for impurity pairs using the LDA total energies (the results will be analyzed in terms of strain energies obtainable via VFF).

III. RESULTS

A. Relaxed geometries and their symmetry groups

While substitution of a single N by As (P) leads to four identical Ga-As (Ga-P) bond lengths (Table II), substitution of *two* N atoms by two As (P) atoms leads to symmetry breaking and to a distribution of Ga-As (Ga-P) bonds. Figure 2 shows schematically the relaxed atomic geometries of the six impurity pairs whose anion-cation bond lengths of types *a*, *b*, *c*, *d*, *e*, and *f* are given in Tables IV and V. For As-As pairs with $n=1,2,4,6$ both LDA and VFF results are shown for several supercell sizes. For P-P pairs only VFF results using 512 atom supercell are shown. Comparison between the VFF 512 atom supercell results for As-As and P-P pairs reveals similar behavior for both impurity systems. Therefore, in the following we concentrate only on the As-As pairs.

Analysis of the relaxed geometries provides the symmetry groups given in Table I (see also labels in Fig. 2). We see that the difference between the symmetry-distinct bonds is largest for $n=1$ and $n=4$, small for $n=6$, and absent for $n=5$. The largest deviation from the tetrahedral geometry occurs for $n=1$, where for As-As (P-P) pairs the *b* bonds are expanded by 0.2 (0.3) % and the *c* bonds are contracted by 0.9 (0.8) % with respect to the bond length for isolated impurities (values corresponding to the VFF 512 atom calculations).

To check the finite size effects, VFF calculations with supercells up to 13 824 atoms ($12\times12\times12$ eight atom unit cells) were used. The changes in the bond lengths even between large 512 and 13 824 atom supercells indicate that the

TABLE IV. Bond lengths for GaN:As_2. The relative bond lengths $R^{\alpha}_{\text{Ga-As}}/R^{0}_{\text{Ga-N}}$ are grouped into six types $\alpha=a,b,c,d,e,f$ (see Fig. 2) describing the atomic configuration of the $n=1,2,3,4,5,6$ As-As pairs. The values for isolated impurity are also given. The VFF results with 64, 216, 512, and 13 824 atom supercells are compared with LDA 64 and 216 atom supercell calculations for As-As pairs.

	Bond *a*	Bond *b*	Bond *c*	Bond *d*	Bond *e*	Bond *f*
$n=1$ pairs						
LDA 64	1.147	1.157	1.158			
LDA 216	1.155	1.165	1.165			
VFF 64	1.136	1.146	1.133			
VFF 216	1.144	1.153	1.140			
VFF 512	1.146	1.154	1.141			
VFF 13 824	1.147	1.156	1.142			
$n=2$ pairs						
LDA 216	1.159	1.162				
VFF 216	1.148	1.150				
VFF 512	1.149	1.152				
VFF 13 824	1.150	1.153				
$n=3$ pairs						
VFF 512	1.152	1.152	1.153	1.153	1.152	1.149
VFF 13 824	1.153	1.153	1.154	1.154	1.153	1.150
$n=4$ pairs						
LDA 216	1.153	1.159	1.154			
VFF 216	1.143	1.148	1.145			
VFF 512	1.145	1.150	1.147			
VFF 13 824	1.146	1.151	1.148			
$n=5$ pairs						
VFF 512	1.151	1.151	1.151	1.151	1.151	1.151
VFF 13 824	1.152	1.152	1.152	1.152	1.152	1.152
$n=6$ pairs						
LDA 216	1.160	1.158	1.160	1.160		
VFF 216	1.149	1.148	1.148	1.149		
VFF 512	1.150	1.151	1.149	1.151		
VFF 13 824	1.151	1.152	1.150	1.152		
$n\rightarrow\infty$ (isolated)						
LDA 64	1.155					
LDA 216	1.160					
VFF 64	1.145					
VFF 216	1.150					
VFF 512	1.151					
VFF 13 824	1.151					

TABLE V. Bond lengths for GaN:P_2. The relative bond-lengths $R^{\alpha}_{\text{Ga-P}}/R^{0}_{\text{Ga-N}}$ grouped into four types $\alpha = a,b,c,d,e,f$ (see Fig. 2) describing the atomic configuration of the N_i, $i=1,2,3,4,5,6$ P-P pairs. The values for isolated impurity are also given. Only VFF results with 512 atom cell are given due to the analogous behavior with As-As pairs.

	Bond *a*	Bond *b*	Bond *c*	Bond *d*	Bond *e*	Bond *f*
$n=1$	1.125	1.134	1.122			
$n=2$	1.130	1.132				
$n=3$	1.132	1.132	1.133	1.133	1.132	1.129
$n=4$	1.126	1.130	1.128			
$n=5$	1.131	1.131	1.131	1.131	1.131	1.131
$n=6$	1.131	1.131	1.130	1.131		
$n\rightarrow\infty$ (isolated)	1.131					

impurity-induced atomic displacements (strain fields) have a long-range character. (This will be addressed further in Sec. III E). Qualitatively the atomic relaxations even with the smallest system size (64 atoms) are consistent with the largest (13 824 atoms) supercell.

Comparison between LDA and VFF bond lengths for As-As pairs with $n=1,2,4,6$ indicates good agreement between the two methods, as discussed already for $n=1$ in Sec. II B. We next investigate how the energy level structure reflects these reduced symmetries.

B. Single-particle energy levels and wave functions

An isolated As or P impurity in GaN produces a t_2^6 level inside the gap, occupied by six electrons.[6] Figures 4 and 5 show the single-particle energy levels of As-As and P-P pairs in GaN as calculated using the EPM. The most prominent fact in Figs. 4 and 5 is that the degenerate t_2 triplet found for the isolated impurities is split for all impurity pairs studied. According to group theory, any *l*-fold degeneracy bears a one-to-one correspondence to the existence of a *l*-dimensional irreducible representation of the specific symmetry group.[27] Observation of the first column in the character tables of C_{2v}, C_S, and C_2 (Refs. 27 and 28) shows that for all of these symmetry groups, the irreducible representations are *one* dimensional. This predicts singly-degenerate single-particle levels in the case of $n=1$ (C_{2v}), $n=3$ (C_s), and $n=5$ (C_2) pairs, consistent with the EPM results presented in Figs. 4 and 5. For $n=2$ (D_{2d}) and $n=6$ (C_{3v})

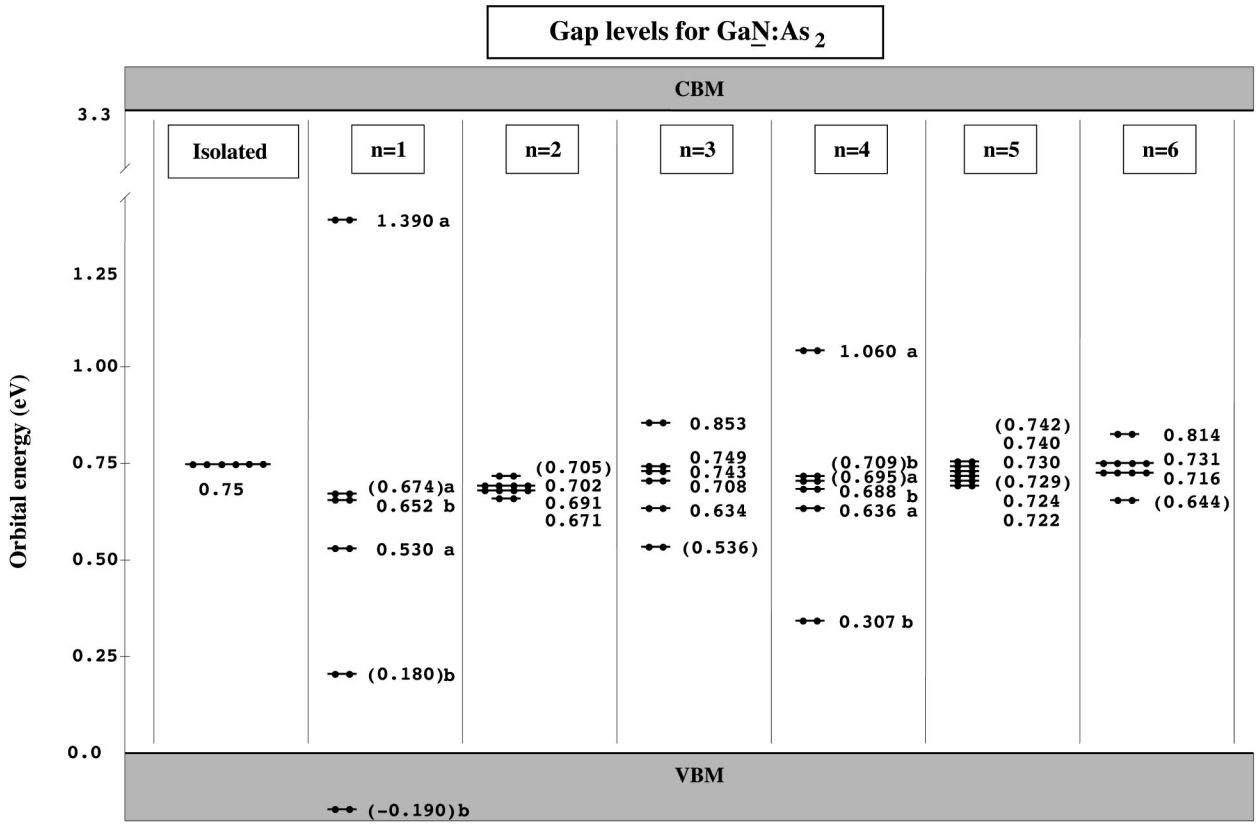

FIG. 4. The single-particle levels calculated by the EPM for the $n=1,2,3,4,5,6$ As-As impurity pairs. For comparison, the data for an isolated As-impurity is shown on the left. For $n=5$ the result corresponding to the 1000 atom supercell calculation is shown, for other cases the results correspond to 512 atom supercells. Numbers give energies in eV with respect to the valence band maximum. Numbers in parentheses denote levels whose dipole matrix element to the CBM [Eq. (1)] is small.

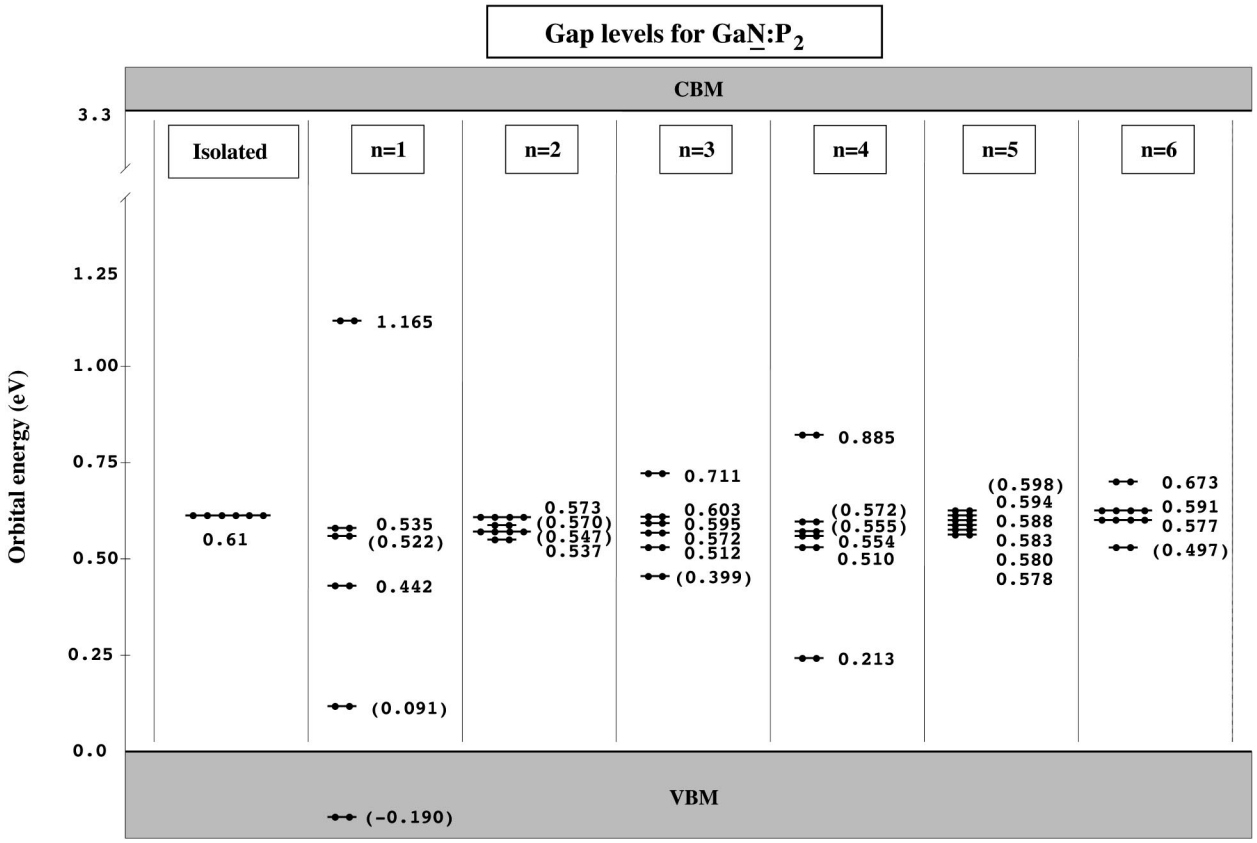

FIG. 5. The single-particle levels calculated by the EPM for the $n=1,2,3,4,5,6$ P-P impurity pairs. For comparison, the data for an isolated P impurity is shown on the left. The results correspond to 512 atom supercells. Numbers give energies in eV with respect to the valence band maximum. Numbers in parentheses denote levels whose dipole matrix element to the CBM [Eq. (1)] is small.

there is only a partial lifting of the degeneracy, consistent with the two-dimensional representation found in character tables for these symmetry groups.[27]

The magnitude of level splitting is largest for $n=1$ and $n=4$ pairs with C_{2v} symmetry. The larger interatomic separation for the $n=4$ pair (Table I) reduces the interaction between the t_2 triplets and thus leads to smaller energy level splitting than for the $n=1$ pair. In general, the energy level splitting shows a nonmonotonic behavior as a function of the pair separation d. This demonstrates the exceptional orientational dependence of the t_2-t_2 interaction.

For As-As pair $n=5$ (C_2 symmetry) the splitting is only about 20 meV, implying a minor interaction between the impurity atoms. The given single-particle levels are derived using a 1000 atom supercell. With a 512 atom supercell the levels split into three nearly (within 0.5 meV) twofold degenerate levels. According to the character table of C_2 symmetry, no degeneracy should be exhibited, which is consistent with the 1000 atom supercell result. The observed minor difference between the 512 and 1000 atom supercells suggests that in the limit of well-separated weakly interacting impurities even a 512 atom supercell cannot fully exclude the interaction between periodic images. For consistency, we have checked the consistency of our results with the 1000 atom supercell for other impurity pairs as well, and the results are in good agreement with the 512 atom calculation.

Figure 6 illustrates the electronic wave functions of the six impurity levels of the As-As $n=1$ pair. The orbitals are labeled in order of increasing energies, following Fig. 4. The lowest energy orbital with $\epsilon=\epsilon_v-0.190$ eV resides inside the valence band and is identified based on the localization at the impurity pair. Analysis of this defect level based on the behavior of wave function sign under symmetry operations[28] shows that it can classified as a_1 orbital. The other five impurity levels shown in Fig. 6 can be classified as b_1, a_1, b_2, a_2, and b_1 orbitals, in order of increasing energy. Similar classification is straightforward to construct for the orbitals related other impurity pairs. The results are shown in Table VI.

Further analysis[29] of the single-particle states for $n=1$ pair reveals that the lowest orbital (inside the valence band) has a bonding character while the uppermost orbital is antibonding. The bonding (antibonding) character for all the orbitals in the case of $n=1$ and $n=4$ As-As pairs is shown with b (a) in Figs. 4 and 6. This characterization will be used below (Sec. III E) to explain the trends in formation energies for the $n=1$ and $n=4$ pairs.

Comparison between the results for As-As and P-P pairs in Figs. 4 and 5 reveals a very similar behavior of the single-particle levels. However, a minor difference in the order of single-particle levels in the case of $n=3$ in apparent. The energy levels largely obey the trend observed for isolated impurities, i.e., the As-As-induced levels reside deeper in the band gap than the P-P-related levels.

C. Transition probabilities

Given the significant level splitting due to the impurity-impurity interaction (Figs. 4 and 5), it is interesting to find

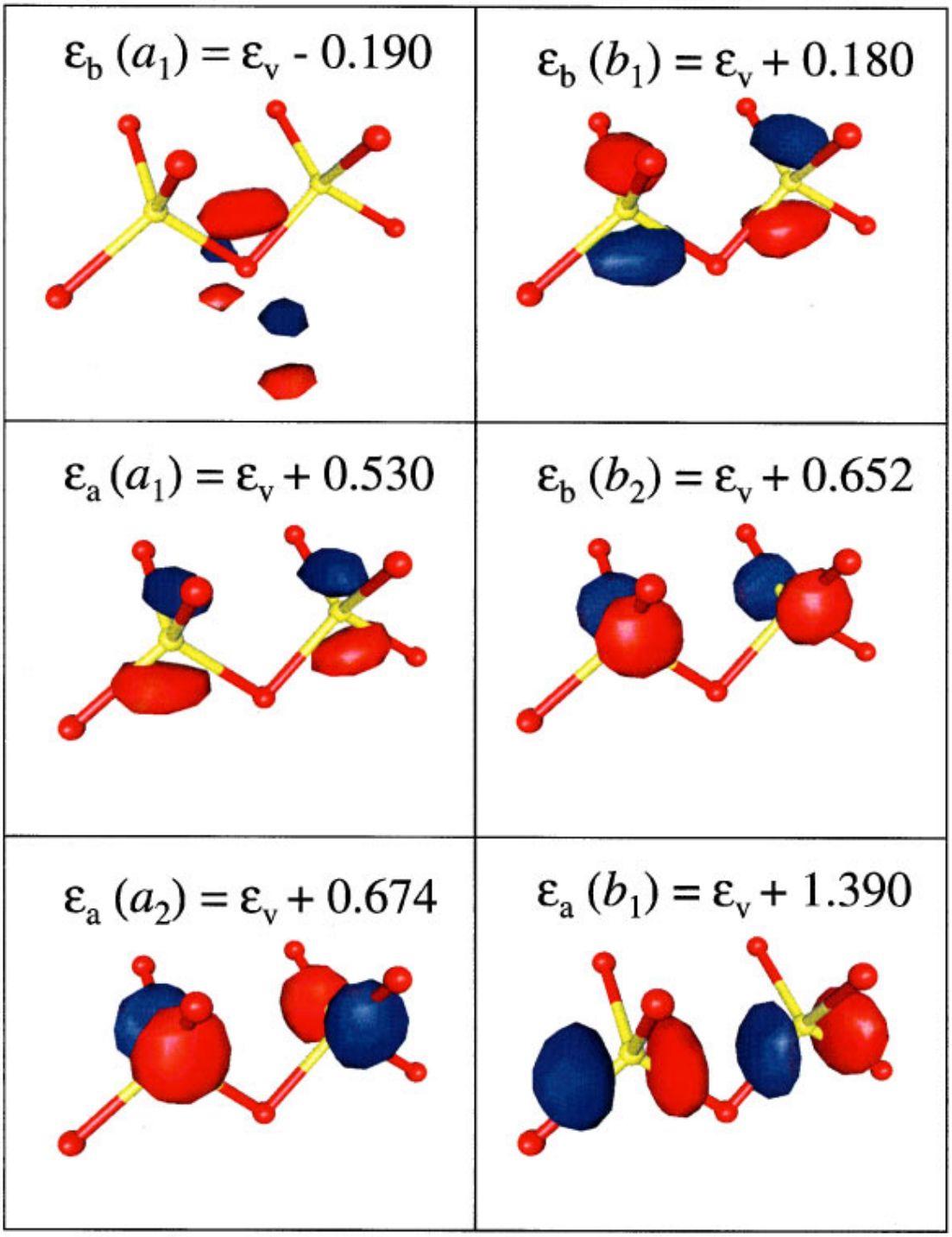

FIG. 6. (Color) The wave functions of the impurity orbitals for $n=1$ As-As pair. The orbitals correspond to the EPM calculation with 512 atom supercell. The wave functions are illustrated as isosurfaces drawn at approximately half of the maximum amplitude. The red (blue) isosurface corresponds to positive (negative) wave function sign. The yellow (red) atoms correspond to As (Ga) atoms. The subscripts *a* and *b* denote antibonding and bonding orbitals, respectively. a_1, a_2, b_1, and b_2 are symmetry representations in C_{2v} (Table VI).

the transition probabilities between these defect-related split levels and the conduction band. We have thus calculated the (normalized) dipole matrix elements

$$p_\alpha = \frac{|\langle \psi_{\mathrm{CBM}}|\mathbf{p}|\psi_\alpha\rangle|^2}{|\langle \psi_{\mathrm{CBM}}|\mathbf{p}|\psi_{\mathrm{VBM}}\rangle|^2} \tag{1}$$

between the lowest conduction band (from the defect-free bulk calculation) and the defect levels α, normalizing the values with respect to the direct CBM to VBM transition matrix element in pure GaN. The wave functions are obtained using the EPM and 512 atom supercells. The values for p_α for each n pair are given in Table VII. The dipole matrix for the transition from CBM to defect level of the isolated impurity is 0.05 (0.15 taking the threefold degeneracy into account). Comparing the values in Table VII with this isolated limit we see that the probability for an electronic transition from the CBM into the highest single-particle level

TABLE VI. Classification of single-particle orbitals (O_i) encountered for impurity-pairs based on group theory. The orbitals are labeled in order of increasing energy (see Figs. 4, 5, and 6). The doubly degenerate e orbitals are indicated with e^* and e^{**}.

As-As pairs	O_1	O_2	O_3	O_4	O_5	O_6
$n=1$	a_1	b_1	a_1	b_2	a_2	b_1
$n=2$	b_2	e^*	e^*	e^{**}	e^{**}	a_1
$n=3$	a'	a''	a'	a''	a'	a'
$n=4$	a_1	a_1	b_2	b_1	a_2	b_1
$n=5$	a	b	a	b	a	b
$n=6$	a_1	e^*	e^*	e^{**}	e^{**}	a_1
P-P pairs	O_1	O_2	O_3	O_4	O_5	O_6
$n=1$	a_1	b_1	a_1	a_2	b_2	b_1
$n=2$	b_2	e^*	e^*	a_1	e^{**}	e^{**}
$n=3$	a'	a''	a'	a''	a'	a'
$n=4$	a_1	a_1	b_2	b_1	a_2	b_1
$n=5$	a	a	b	b	a	b
$n=6$	a_1	e^*	e^*	e^{**}	e^{**}	a_1

in the case of $n=1$ and $n=4$ pairs is substantial. Thus we predict that the corresponding emission energies (distinctive from the isolated impurity) should be detectable in photoluminescence experiments for $n=1$ pairs; we show in Sec. III E that $n=4$ pairs are thermodynamically unstable and therefore the experimental verification of their optical character may be more complicated.

D. Exciton binding energy

In Ref. 6 it was shown that the $(+/0)$ ionization level can be identified as the exciton binding energy:

TABLE VII. The normalized dipole matrix elements p_α [see Eq. (1)] for optical transitions between the lowest conduction band level (CBM) and defect orbital α (Figs. 4 and 5). The normalization is done with respect to the CBM to VBM transition in pure GaN. The defect orbitals are labeled in order of increasing energy (see Figs. 4, 5, and 6). For degenerate levels (Figs. 4 and 5) the total transition matrix element can be obtained by summing the values of constituent levels. Matrix elements smaller than 10^{-7} are indicated with an asterisk (forbidden transitions under electric-dipole selection rules).

As-As	p_1	p_2	p_3	p_4	p_5	p_6
$n=1$	8×10^{-4}	1×10^{-4}	0.10	0.09	*	0.03
$n=2$	0.10	0.01	0.01	0.08	0.08	*
$n=3$	5×10^{-5}	0.09	0.06	0.01	0.04	0.06
$n=4$	0.02	0.10	0.10	2×10^{-3}	*	0.05
$n=5$	0.08	0.09	4×10^{-3}	0.09	0.02	9×10^{-4}
$n=6$	6×10^{-5}	0.07	0.07	0.02	0.02	0.07
P-P	p_1	p_2	p_3	p_4	p_5	p_6
$n=1$	5×10^{-4}	2×10^{-4}	0.12	*	0.11	0.04
$n=2$	0.12	1×10^{-3}	1×10^{-3}	*	0.11	0.11
$n=3$	5×10^{-5}	0.11	0.07	0.02	0.05	0.08
$n=4$	0.02	0.12	0.12	2×10^{-3}	*	0.06
$n=5$	0.10	0.04	0.07	0.11	0.02	1×10^{-3}
$n=6$	5×10^{-5}	0.09	0.09	0.03	0.03	0.09

$$E_b \equiv E_{\text{gap}} - E_{\text{ZPL}} = \epsilon(+/0), \tag{2}$$

where E_{gap} is the band gap energy and E_{ZPL} is the zero phonon line energy. The ionization level can be determined based on the total energies for neutral (E_0) and singly positive (E_+) impurities in a LDA supercell calculation as $\epsilon(+/0)=E_0-E_+$, avoiding thus the LDA band gap error in the estimate. Here E_b for the $n=1$ pair is determined analogously: based on the LDA total energies of fully relaxed the neutral and singly positive systems we can determine the position of the $(+/0)$ ionization levels. Our result using the 64 atom cell for the nearest-neighbor pairs and isolated impurities[6] are

$$E_b(\text{As-As}) = 1.27 \text{ eV}, \quad E_b(\text{P-P}) = 0.85 \text{ eV},$$
$$E_b(\text{As}) = 0.41 \text{ eV}, \quad E_b(\text{P}) = 0.22 \text{ eV}. \tag{3}$$

Our results thus predict that the exciton binding energy for the nearest-neighbor pair is three to four times larger than for the isolated impurity. This result is in agreement with the experimental and theoretical results on analogous system of CdS:Te.[32–34] Experimental testing of our predictions [Eq. (3)] are called for.

E. Impurity pair formation energies

Having demonstrated the exceptional interaction and optical properties of the deep t_2 defect orbitals *assuming* the presence of As-As or P-P impurity pairs in GaN, we next inquire what is the energetics involved in finding two impurity atoms at nearby nitrogen sublattice sites. Of course, for studying impurity-impurity interaction one needs to assure that there is sufficient solubility in the first place. Experiments indeed show[1–3] that there *exists* a finite concentration of As or P impurities in GaN. Although their concentration is limited by large (positive) heat of solution for $GaN_{1-x}P_x$ and $GaN_{1-x}As_x$ alloys,[35] it has been shown experimentally that significant concentrations (10^{17}–10^{18} $1/cm^3$) of these impurities can be incorporated in GaN.[1–3] We thus study the question, given that impurities *can* be introduced, do they attract or repel each other? In this purpose we calculate the bulk pair formation energy $\Delta E^{(n)}$ as the difference between the total energy of two nth neighbor impurities and for two impurities at infinite separation (twice the energy of an isolated impurity), i.e.,

$$\begin{aligned}\Delta E^{(n)} &\equiv E^{(n)} - E^{(n\to\infty)} \\ &= [E(\text{Ga}_{m/2}\text{N}_{(m/2-2)}X_2) + E(\text{Ga}_{m/2}\text{N}_{m/2})] \\ &\quad - 2E(\text{Ga}_{m/2}\text{N}_{(m/2-1)}X),\end{aligned} \tag{4}$$

where n denotes the pair index, $X=$P, As, and m is the number of atoms in the supercell. The energies in the second line in Eq. (4) correspond to the fully relaxed supercell calculations with atomic occupation given in the parentheses. In LDA calculations an identical k-point sampling is applied for all three total-energy values for consistency. The lattice parameter for all supercells has been chosen to correspond to the theoretical bulk GaN lattice constant.[30]

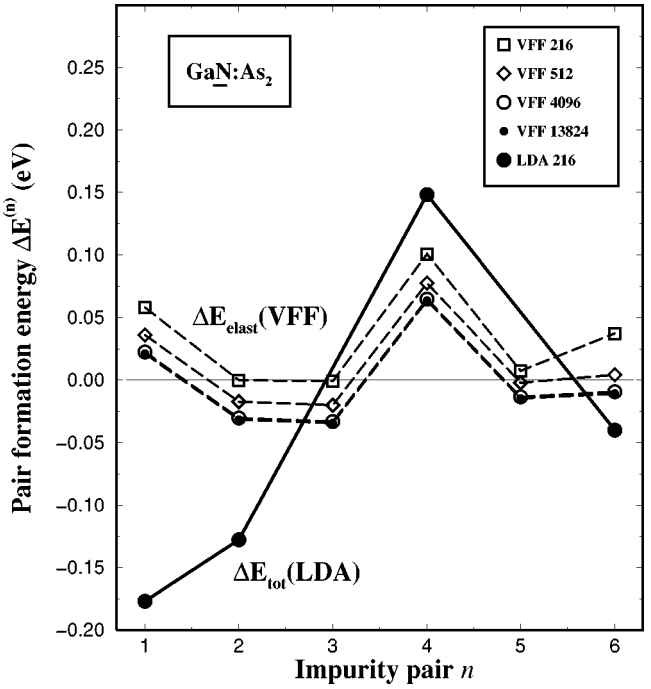

FIG. 7. The pair interaction energies $\Delta E^{(n)}$ [Eq. (4)] for $n=1,2,3,4,5,6$ As-As pairs. The VFF calculations include only elastic contribution to the strain energy, while LDA results contain also chemical effects, as described in Sec. III E. The supercell sizes are denoted by the total number of atoms $M=216$, 512, 4096, 13 824 corresponding to $(3\times3\times3)$, $(4\times4\times4)$, $(8\times8\times8)$, $(12\times12\times12)$ stacking of eight atom zinc blende unit cells, respectively.

1. Total formation energy

The 216-atom/cell LDA calculated total pair formation energies $\Delta E^{(n)}$ for the As-As pairs are shown as solid line in Fig. 7. The result for $\Delta E^{(n=1)}$ is negative (-0.18 eV). $\Delta E^{(n=2)}$ is slightly higher than $\Delta E^{(n=1)}$, but remains negative indicating binding between the impurity atoms.[36] For $\Delta E^{(n=4)}$ we find a large positive value suggesting that the $n=4$ configuration is unstable with respect to dissociation. $\Delta E^{(n=6)}$ is found to have a small negative value indicating only minor interaction between the impurities. Thus, our results predict clear association for $n=1,2$ and dissociation for $n=4$.

To understand the trends with $\Delta E^{(n)}$ as a function of n and to study the system size dependence we decompose $\Delta E^{(n)}$ into an elastic strain part $\Delta E^{(n)}_{\rm elast}$, and a chemical part $\Delta E^{(n)}_{\rm chem}$:

$$\Delta E^{(n)}=\Delta E^{(n)}_{\rm elast}+\Delta E^{(n)}_{\rm chem}. \tag{5}$$

The self-consistent LDA calculations include both elastic and chemical contribution to the formation energy. The purely elastic strain energy part $\Delta E^{(n)}_{\rm elast}$ is modeled by the VFF method which, by construction, has only deformation terms, but no charge-transfer or orbital-dependent terms. Thus, $\Delta E^{(n)}_{\rm elast}$ is given by Eq. (4) with the total energies E corresponding to $E_{\rm VFF}$. Due to the good agreement between the LDA and VFF bond lengths (Table IV) we can use $\Delta E^{(n)}_{\rm elast}$ given by VFF to estimate the magnitude of chemical part in LDA calculations as $\Delta E^{(n)}_{\rm chem}=\Delta E^{(n)}_{\rm LDA}-\Delta E^{(n)}_{\rm VFF}$. Furthermore, due to the low computational cost in VFF calculations, we can investigate the convergence of the elastic energy as a function of system size using large supercells.[37]

2. The elastic contribution

The elastic contribution $\Delta E^{(n)}_{\rm elast}$ is shown as dashed lines in Fig. 7. The absolute magnitude of $\Delta E^{(n)}_{\rm elast}$ converges slowly as a function of the supercell size m; only the $m=4096$ atom supercell results are nearly indistinguishable from the $m=13\,824$ atom system. However, the relative energies between different n's in $\Delta E^{(n)}$ remain nearly identical. The slow convergence of the absolute values with m indicates a long-range interaction of the strain fields induced by the two impurities. This is expected from the classic solution for a spherical inclusion in an isotropic matrix with nonequal lattice parameter:[31] the elastic displacement decays as a power law (the inverse square of the distance from the center of distortion).

$\Delta E^{(n)}_{\rm elast}$ (with the converged system size $m=13\,824$) is positive for $n=1$ and $n=4$ pairs (C_{2v} symmetry), indicating repulsive elastic interaction between the impurity atoms at these positions. For $n=2$, 3, 5, and 6 we find small *negative* values for $\Delta E^{(n)}_{\rm elast}$ corresponding to attractive interaction between the As atoms. These results are similar to the VFF results for nitrogen impurity pairs in GaAs.[26] Thus, the elastic interaction energies would suggest that As-As pairing avoids $n=1$ and $n=4$ neighbor shells and favors $n=2$ and $n=3$ configurations.

3. Chemical contribution

The chemical contribution $\Delta E^{(n)}_{\rm chem}=\Delta E^{(n)}_{\rm LDA}-\Delta E^{(n)}_{\rm elast}$ plays an important role in determining the pair interaction energy. For consistency, the $m=216$ atom cell size is used both for $\Delta E^{(n)}_{\rm LDA}$ and $\Delta E^{(n)}_{\rm VFF}$ when calculating $\Delta E^{(n)}_{\rm chem}$. In particular, the chemical energy is -0.23 eV for $n=1$, -0.13 eV for $n=2$, and small for larger n. In order to understand this we analyze the interaction of the deep t_2 defect orbitals. As explained in Sec. III B and Fig. 4 the t_2-t_2 interaction leads to large splitting of the defect energy levels. The largest splitting of the triply degenerate gap levels was seen to occur in the case of $n=1$ pair (Fig. 4), while a smaller splitting occurred for the $n=4$ pair due to larger distance between the impurity atoms. As discussed in Sec. III B and Fig. 4 the lowest orbital has a bonding character while the uppermost orbital is antibonding for both $n=1$ and $n=4$ pairs. The ''center of mass'' for the bonding-antibonding orbitals of $n=1$ pair can be seen to be considerably *lower* than the position of the deep level of the isolated impurity, while for the $n=4$ pair the corresponding average is only slightly below the isolated value. This indicates that the orbitals for the $n=1$ pair induce a significant bonding contribution while the corresponding effect due to orbitals for the $n=4$ is much smaller. The calculated values for $\Delta E^{(n)}_{\rm chem}$ above indeed confirm this expectation.

Thus, the calculated values for $\Delta E^{(n)}$ predict that, if we assume a thermal equilibrium during the growth process, the As impurities should favor pairing into $n=1$ and $n=2$ nearest and next-nearest neighbor configurations rather than be evenly (randomly) distributed. For P impurity pair we expect

a similar behavior based on the analogous single-particle orbital energies and atomic geometries.[38]

IV. CONCLUSIONS

The self-consistent plane-wave pseudopotential and empirical pseudopotential methods are used to study As-As and P-P substitutional impurity pairs in GaN. The results demonstrate an unconventional interaction between the impurity atoms.

We show that the interaction between localized impurity-induced t_2 triplets leads to a large splitting of the degenerate defect levels, which strongly depends on the orientation of the impurity pair with respect to the lattice. The largest splitting is predicted for the $n=1$ and $n=4$ pairs exhibiting C_{2v} symmetry, while only a small level splitting is found for $n=2$ pairs (D_{2d} symmetry). The calculated dipole matrix elements for transitions between these defect levels and lowest conduction band predict the existence of rich spectroscopic series associated with the pairing of the impurity atoms. The exciton binding energies for $n=1$ As-As (P-P) impurity are calculated to be 1.27 (0.85) eV which are significantly larger than the values for isolated impurities (0.41 eV for As and 0.22 eV for P). These results await experimental confirmation.

It is shown that the interaction of the deep electronic orbitals plays an important role in determining the pair formation energies in addition to the interaction of impurity induced strain fields. The calculated pair formation energies indicate that incorporation of two impurity atoms at the nearest or next-nearest fcc-lattice sites is energetically favorable compared with an infinite separation. In contrast, the fourth neighbor configuration is found to be unstable with respect to dissociation. An important computational detail is that the pair formation energies are found to be highly sensitive to the supercell size applied in the calculations.

ACKNOWLEDGMENTS

T.M. gratefully acknowledges the financial support provided by the Väisälä Foundation (Helsinki, Finland). This work was supported in part by the U.S. Department of Energy, OER-BES-DMS, Grant No. DE-AC36-83-CH10093.

*Electronic address: tmattila@nrel.gov
†Electronic address: alex_zunger@nrel.gov

[1] X. Li, S. Kim, E. E. Reuter, S. G. Bishop, and J. J. Coleman, Appl. Phys. Lett. **72**, 1990 (1998).
[2] L. J. Guido, P. Mitev, M. Gherasimova, and B. Gaffey, Appl. Phys. Lett. **72**, 2005 (1998).
[3] W. M. Jadwisienczak and H. J. Lozykowski (unpublished).
[4] L. Bellaiche, S.-H. Wei, and A. Zunger, Phys. Rev. B **54**, 17 568 (1996).
[5] L. Bellaiche, S.-H. Wei, and A. Zunger, Appl. Phys. Lett. **70**, 3558 (1997).
[6] T. Mattila and A. Zunger, Phys. Rev. B **58**, 1367 (1998).
[7] J. I. Pankove and J. A. Hutchby, J. Appl. Phys. **47**, 5387 (1976).
[8] R. D. Metcalfe, D. Wickenden, and W. C. Clark, J. Lumin. **16**, 405 (1978).
[9] T. Ogino and M. Aoki, J. Appl. Phys. **18**, 1049 (1979).
[10] D. G. Thomas, J. J. Hopfield, and C. J. Frosch, Phys. Rev. Lett. **15**, 857 (1965).
[11] B. Gil, Physica B **146**, 84 (1987).
[12] J. Ihm, A. Zunger, and M. L. Cohen, J. Phys. C **12**, 4409 (1979).
[13] J. Perdew and A. Zunger, Phys. Rev. B **23**, 5048 (1981).
[14] D. Vanderbilt, Phys. Rev. B **41**, 7892 (1990); K. Laasonen, A. Pasquarello, R. Car, C. Lee, and D. Vanderbilt, *ibid.* **47**, 10 142 (1993).
[15] G. B. Bachelet, D. R. Hamann, and M. Schüter, Phys. Rev. B **26**, 4199 (1982); D. R. Hamann, *ibid.* **40**, 2980 (1989). Our pseudopotentials are verified to be ghost-free using the method by X. Gonze, R. Stumpf, and M. Scheffler, *ibid.* **44**, 8503 (1991).
[16] S. G. Louie, S. Froyen, and M. L. Cohen, Phys. Rev. B **26**, 1738 (1982).
[17] The use of Ga $3d$ electrons as part of core states is motivated by previous studies which have shown general agreement between defect properties (formation energies, ionization levels) calculated treating Ga $3d$ orbitals as part of valence states (Ref. 18) and as part of core (Ref. 19) provided that the nonlinear core-valence exchange-correlation scheme (Ref. 16) is applied.
[18] J. Neugebauer and C. G. Van de Walle, Phys. Rev. B **50**, 8067 (1994).
[19] T. Mattila and R. M. Nieminen, Phys. Rev. B **55**, 9571 (1997).
[20] H. J. Monkhorst and J. D. Pack, Phys. Rev. B **13**, 5188 (1976).
[21] M. J. Puska, S. Pöykkö, M. Pesola, and R. M. Nieminen, Phys. Rev. B **58**, 1318 (1998).
[22] See, e.g., Ref. 13. The band gap obtained for zinc blende GaN in our LDA calculations is 2.67 eV, while the experimental value is 3.3 eV. The band gap is calculated at the theoretical lattice constant of 4.39 Å; the experimental value is 4.52 Å.
[23] P. N. Keating, Phys. Rev. **145**, 637 (1966).
[24] R. M. Martin, Phys. Rev. B **1**, 4005 (1970).
[25] L.-W. Wang and A. Zunger, J. Chem. Phys. **100**, 2394 (1994).
[26] L. Bellaiche and A. Zunger, Phys. Rev. B **57**, 4425 (1998).
[27] J. F. Cornwell, *Group Theory and Electronic Energy Bands in Solids* (North-Holland, Amsterdam, 1969).
[28] D. F. Shriver, P. Atkins, and C. H. Langford, *Inorganic Chemistry*, 2nd ed. (Freeman, New York, 1994).
[29] When moving the impurity atoms closer to each other the bonding (antibonding) orbital energy is seen to decrease (increase).
[30] In VFF calculations $R^0_{\text{Ga-N}}$ is equal to the experimental value 4.52 Å, while in the LDA calculations the bulk bond length is 4.39 Å due to the overbinding in LDA (Ref. 6).
[31] J. D. Eshelby, J. Appl. Phys. **25**, 255 (1954).
[32] D. M. Roessler, J. Appl. Phys. **41**, 4589 (1970).
[33] O. Goede and D. Hennig, Phys. Status Solidi B **119**, 261 (1983).
[34] M. Hanke, D. Hennig, and A. Kaschte, Phys. Status Solidi B **143**, 655 (1987).
[35] Our calculated values for the ''interaction parameter'' Ω in the heat of solution $\Delta H=\Omega x(1-x)$ are 2.2 eV (2.6 eV) per anion for $GaN_{1-x}P_x$ ($GaN_{1-x}As_x$).
[36] $\Delta E^{(n)}$ converge slowly as a function of supercell size. In LDA calculations we find $\Delta E^{(n=1)}$ $+0.14$ and -0.18 eV for $m=64$ and $m=216$, respectively. Using VFF the corresponding values are $+0.14$ and $+0.06$ eV.
[37] A remaining question is how well $\Delta E^{(n)}$ is converged in the 216 atom LDA calculations with respect to the system size. Based on the VFF results for the *elastic* interaction we expect that a larger system size in LDA calculations would merely result in a small

($\leqslant 0.05$ eV) and nearly constant decrease in the interaction energy for all impurity pairs due to the shift in $\Delta E^{(n)}_{\text{elast}}$. This shift would not alter the qualitative picture. It is more difficult to estimate the convergence of the chemical interaction $\Delta E^{(n)}_{\text{chem}}$. We have estimated this by comparing results with 64 and 216 atom cells for the isolated As impurity: the energy needed to substitute a N atom with an As atom agrees within 0.05 eV between the two system sizes. This indicates reasonable convergence for the isolated impurity already with 64 atom cell. Based on this observation, we believe that the interaction between the periodic images of the localized orbitals in the case of impurity pairs is not likely to affect the results significantly with the 216 atom cell.

[38] In LDA calculations with the 64 atom supercell for $n=1$ P-P pair we find a value of $\Delta E^{(n=1)}=+0.10$ eV which is slightly smaller than the corresponding value for the $n=1$ As-As pair $+0.14$ eV.